

Gas management in flow field design using 3D direct methanol fuel cell model under high stoichiometric feed

Valeri A. Danilov, Jongkoo Lim, Il Moon[†] and Kyoung Hwan Choi*

Department of Chemical Engineering, Yonsei University, 134 Shinchon-dong, Seodaemun-gu, Seoul 120-749, Korea

*Samsung Advanced Institute of Technology, Suwon 440-600, Korea

(Received 9 February 2006 • accepted 4 May 2006)

Abstract—This study presents a 3D CFD model for modeling gas evolution in anode channels of a DMFC under high stoichiometric feed. The improved two-phase model includes a new submodel for mass source and interphase transfer in anode channels. Case studies of typical flow field designs such as parallel and serpentine flow fields illustrate applications of the CFD model. Simulation results reveal that gas management of typical flow fields is ineffective under certain operating conditions. The CFD-based simulations are used to visualize and to analyze the gas evolution and flow patterns in anode channels. The developed CFD model is useful in flow field design for improving gas management in DMFC.

Key words: DMFC, Two-phase Flow, Gas Management, Flow Field Design

INTRODUCTION

Direct methanol fuel cells (DMFC) are considered as a potential energy source to replace batteries for portable electronics due to potentially higher energy density, nearly zero recharge time and ultralow emissions. However, the wide application of DMFC still requires solving some critical problems such as methanol crossover and gas management. Gas management greatly influences the performance of fuel cells. On the anode side, carbon dioxide is produced by electrochemical oxidation of methanol. Inefficient removal of CO₂ bubbles may block anode channels and decrease efficiency of the fuel cells due to the limited mass transport and maldistribution of reactants.

A few papers are devoted to the flow field design and gas management in DMFC. The most complete information on the influence of the whole factors can be obtained from experiments. Argyropoulos et al. [1999] used transparent DMFC to visualize gas evolution and to analyze the flow behavior. They found that increasing the liquid phase inlet flow rate was extremely beneficial for gas removal. Arico et al. [2000] compared the performance of the serpentine (SFF) and interdigitated (IFF) flow field designs. They found that the interdigitated flow field significantly enhanced mass-transport inside DMFC and provided higher maximum power outputs compared to the classical serpentine geometry. Geiger et al. [2000] used neutron radiography for exploring gas evolution patterns in anode flow fields of DMFC. They reported that gas accumulated to a large extent at the inner section of spiral channels and it blocked a considerable part of the active area. Zhao et al. [2005] observed that open ratio and flow channel length significantly influence the fuel cell performance and pressure drop in the case of single serpentine and parallel flow field designs. Yang et al. [2004] measured two-phase flow pressure drop in the anode flow field of a DMFC. The experimental

results revealed that the pressure drop became almost independent of the current density when the methanol solution flow rate was sufficiently high. Bewer et al. [2004] presented a new experimental method for studying gas evolution in a test cell made of perspex. The method is based on the decomposition of hydrogen peroxide solution (H₂O₂) to oxygen and water in aqueous media. Argyropoulos et al. [2000] developed a pressure drop model for a DMFC and analyzed the effects of various operation parameters on the pressure drop behavior.

Most published models are models of the fuel cell. Baxter et al. [1999] developed a one-dimensional model of a liquid-feed DMFC for transport and electrochemical processes in the single-phase anode catalyst layer. Sundmacher et al. [2001] developed a lumped parameter model for studying the steady state and dynamic behavior of a DMFC. Kulikovskiy developed a simple one-dimensional model of the flow with bubbles in the anode channel of a DMFC. The author indicates large potential for improving the DMFC performance by proper “bubbles management” in the anode side flow field.

Complex anode flow field design requires a 3D DMFC model in order to accurately simulate the gas evolution and mass transfer. This study addresses a model development for simulating the gas-liquid flow and gas evolution in anode channels. The improved two-phase model includes a new submodel for interface mass transfer in anode channels without using empirical correlation. The model is implemented in a computational fluid dynamics (CFD) package to evaluate typical and new flow field designs. The CFD simulations are used to visualize and to analyze the flow patterns and to reduce the number of experiments. A better understanding of these transport processes would provide more efficient gas management and better cell performance.

MODEL FORMULATION

1. Two-Phase Model for Anode Channels

Fluid dynamics and mass transfer processes influence significantly

[†]To whom correspondence should be addressed.

E-mail: ilmoon@yonsei.ac.kr

the gas management and fuel cell performance. Mathematical description of momentum and mass transfer processes in gas-liquid flows is generally based on a two-phase model [Sokolichin and Eigenberger, 1997; Wang and Wang, 2003]. As shown by Triplett et al. [1999], homogeneous model is true for bubbly two-phase flow in microchannels. According to the flow regime maps presented by Yang et al. [2004], bubbly flow occurred in square channel at low volumetric flux of air and high volumetric flux of liquid. The two-phase model in this paper considers anode channels under the following assumptions.

- The two-phase flow is isothermal, incompressible and homogeneous (Newtonian).
- Methanol crossover is neglected.
- Consumption of oxygen in cathode compartment is neglected due to high feeding ratio of air and methanol.

As applied to the anode channels, model equations are given in Table 1.

Mixture parameters - in (1)-(5), the mixture variables and properties are given by

Density	$\rho = \varepsilon_G \rho_G + (1 - \varepsilon_G) \rho_L$
Concentration	$C = C_G \varepsilon_G \rho_G + C_L (1 - \varepsilon_G) \rho_L$
Velocity	$\mathbf{u} = \mathbf{u}_G \varepsilon_G \rho_G + \mathbf{u}_L (1 - \varepsilon_G) \rho_L$
Viscosity	$\mu_{eff} = \mu_G \varepsilon_G + \mu_L (1 - \varepsilon_G)$

where ε_G is gas volume fraction. The model equations for two-phase model in diffusion layer are listed in Table 2.

Details of model variables and mixture properties in the diffusion layer are described by Wang and Wang [2003].

2. Boundary Conditions

The standard boundary conditions are used at channel inlets, exits

Table 1. Governing equations for anode channel

Governing equations	Mathematical expression
Continuity equation ^a	$\nabla \cdot (\rho \vec{u}) = 0$ (1)
Momentum equation ^a	$\nabla \cdot (\rho \vec{u} \vec{u}) = -\nabla P + \nabla \cdot \mathbf{T} + \rho \mathbf{g}$ (2)
Stress tensor ^a	$T_{ij} = \mu_{eff} \left(\frac{\partial u_i}{\partial x_j} + \frac{\partial u_j}{\partial x_i} - \frac{2}{3} \delta_{ij} \frac{\partial u_n}{\partial x_n} \right)$ (3)
Continuity equation for gas phase ^a	$\nabla \cdot (\varepsilon_G \rho_G \vec{u}_G) = \Gamma_G$ (4)
Species conservation ^b	$\nabla \cdot (\rho \vec{u} C^k) = \nabla \cdot ((1 - \varepsilon_G) \rho_L D_{L,eff}^k \nabla C_L^k + \varepsilon_G \rho_G D_{G,eff}^k \nabla C_G^k)$ (5)

^aTaken from Sokolichin and Eigenberger [1997].

^bTaken from Wang and Wang [2003].

Table 2. Governing equations for anode diffusion layer^b

Governing equations	Mathematical expression
Continuity equation	$\nabla \cdot (\rho \vec{u}) = 0$ (6)
Momentum conservation	$\vec{u} = -\frac{k}{\mu_L} (\nabla P + \rho_L \mathbf{g})$ (7)
Species conservation	$\nabla \cdot (\gamma_G \rho \vec{u} C^k) = \nabla \cdot (\rho_L D_{L,eff}^k \nabla C_L^k + \rho_G D_{G,eff}^k \nabla C_G^k) - \nabla \cdot ((C_L^k - C_G^k) \mathbf{j}_L)$ (8)

^bTaken from Wang and Wang [2003].

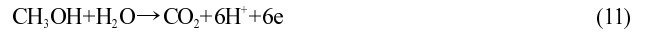
and walls. The detailed boundary conditions are given below. At the inlet of anode flow channels, the boundary values are prescribed from the stoichiometric flow rate and mass fractions:

$$\mathbf{u}|_{inlet} = \mathbf{u}_{in}, \quad C|_{inlet} = C_{in}^{MeOH}, \quad C|_{inlet} = C_{in}^{CO_2} \quad (9)$$

On anode channel walls the no-slip condition and impermeable velocity are applied:

$$\frac{\partial P}{\partial n} = 0, \quad \mathbf{u} = 0 \quad (10)$$

Methanol oxidation includes an electrochemical reaction on catalyst layer and multicomponent mass transfer in diffusion layer. The following electrochemical reactions take place in the fuel cell:



Electrochemical reactions are taken into account by means of boundary conditions at the interface. The next condition of flux continuity is valid for the methanol mass flux at diffusion layer-catalyst layer interface:

$$N_{MeOH}|_{DL} = -M_{MeOH} \frac{1}{6F} \quad (13)$$

The carbon dioxide mass flux at the interface is

$$N_{CO_2}|_{DL} = M_{CO_2} \frac{1}{6F} \quad (14)$$

On the rest walls, no-flux boundary condition is applied for each component:

$$\frac{\partial C^{MeOH}}{\partial n} = 0, \quad \frac{\partial C^{CO_2}}{\partial n} = 0 \quad (15)$$

3. Submodel for Interface Mass Transfer

The mathematical basis of the two-phase model is given by Eqs. (1)-(5). The homogeneous model assumes that the phases move with the same velocity. The presence of bubbles is reflected by gas content ε_G and source term Γ_G . The difficulty in modeling concerns the physical transfer processes taking place across interface such as multicomponent mass transfer.

In accordance with the two-fluid model, gas content is found from continuity Eq. (4). The conventional submodel for estimating the interface mass transfer and the mass source is based on the mass transfer equation [Wang and Wang, 2003]

$$\Gamma_G = \frac{N_{i,G} C_{G,s} + \rho_G \beta_G \Delta C_G}{h} \quad (16)$$

where $N_{i,G}$ -total mass flux transferred from liquid to gas phase; β_G -mass transfer coefficient; ΔC_G -driving force of mass transfer. Mass transfer coefficient from bubbles to the liquid phase is a complicated function of hydrodynamics. A limited number of empirical correlations are available for channels.

It is generally assumed that multicomponent gas phase is in equilibrium with liquid phase. Sundmacher and Scott [1999] and Argyropoulos et al. [2000] showed an application of the equilibrium flash equation for computing gas content under the assumption of complete mixing in anode channel. For given component molar frac-

tions, the local vaporization factor γ is calculated from solving equilibrium flash equation:

$$\sum_{i=1}^3 \frac{(K_i - 1) C_i \frac{M_{mix}}{M_i}}{(K_i - 1) \gamma + 1} = 0 \quad (17)$$

where K_i -the distribution of each component between vapor and liquid phases, $K_i = y_i/x_i$; γ -the local vaporization factor, $\gamma = V/(V+L)$.

Vaporization factor is the ratio of evaporated molar gas flow rate to total flow rate. For anode channel, the carbon dioxide is the product of electrochemical reaction Eq. (11) defined at diffusion layer interface Eq. (14). Concentration of methanol in channel is decreased due to electrochemical reaction Eq. (11) and boundary condition Eq. (13). Gas evolution results from interface mass transfer of carbon dioxide in anode channels. Multicomponent mixture in gas phase includes carbon dioxide, methanol and water in equilibrium with liquid phase. By definition, the source of mass in gas phase in Eq. (4) is

$$\Gamma_G = M_G \frac{\delta G}{\delta V} \quad (18)$$

Another way of estimating interface flux δG in Eq. (18) is to use the equilibrium condition. For volume δV in anode channel in Fig. 1, we define vaporization factor as follows:

$$\gamma = \frac{\delta G}{L + (N_{anode}^{CO_2} / M^{CO_2}) \delta S} \quad (19)$$

where δG -molar flow rate transferred from liquid to gas phase; L -liquid molar flow rate in channel with volume δV ; δS -area, $\delta S = \delta V/h$.

Using equilibrium condition Eq. (19), we suggest the following equation for estimating mass source Γ_G in Eq. (4):

$$\Gamma_G = M_G \gamma \left(\psi + \frac{N_{anode}^{CO_2}}{M^{CO_2} h} \right) \quad (20)$$

where M_G -molecular weight of gas phase; ψ -coefficient, $\psi = L/\delta V$.

Derivation of the auxiliary equation for coefficient ψ is given below. To evaluate the coefficients, we use the total mass balance for gas phase in anode channels,

$$(G_{out} - G_{in}) = \bar{\Gamma}_G V_{anode} \quad (21)$$

where G_{in} -gas flow rate at inlet section, $G_{in}=0$; V_{anode} -volume of anode channels. Gas flow rate at outlet section G_{out} is

$$G_{out} = u_{G,out} \rho_G \varepsilon_{G,out} S_{out} \quad (22)$$

where S_{out} -area of the stream outlet section; $u_{G,out}$ -velocity of gas at

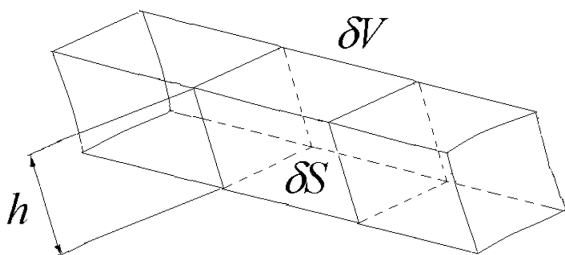


Fig. 1. Control volume of anode channel with volume δV and area δS .

section S_{out} ; $\varepsilon_{G,out}$ -gas content in two-phase stream at section S_{out} .

Mean mass source is

$$\Gamma_G = M_G \bar{\gamma} \left(\psi + \frac{N_{anode}^{CO_2}}{M^{CO_2} h} \right) \quad (23)$$

where $\bar{\gamma}$ -mean fractional vaporization, $\bar{\gamma} = \frac{1}{V_{anode}} \int \gamma dV$.

Finally, solving Eq. (21) and Eq. (23) for ψ we have

$$\psi = \frac{G_{out} - G_{in}}{V_{anode} M_G \bar{\gamma}} - \frac{N_{anode}^{CO_2}}{M^{CO_2} h} \quad (24)$$

It should be noted that the new submodel for mass source Eq. (20) corresponds to an equilibrium model of multicomponent mass transfer between liquid and gas in anode channels [Danilov et al., 2005].

4. Electrokinetics

Using the Tafel equation for methanol oxidation, the anode overpotential is expressed as

$$\eta_A = \frac{RT}{\alpha_A F} \ln \left(\frac{I}{I_0^{MeOH}} \right) \quad (25)$$

where α_A -charge transfer coefficient of the anode. Anode exchange current density is

$$I_0^{MeOH} = I_{0,ref}^{MeOH} \left(\frac{c_{L,MeOH}}{c_{L,threshold}^{MeOH}} \right)^n \quad (26)$$

where $c_{L,threshold}^{MeOH}$ -threshold methanol concentration, $c_{L,threshold}^{MeOH} = 0.1$ M. Electrochemical reaction of methanol oxidation is zero-order ($n=0$) when methanol concentration is higher than $c_{L,threshold}^{MeOH}$.

Cathode overpotential derived from Tafel equation for oxygen reduction at catalyst layer is given by

$$\eta_c = \frac{RT}{\alpha_c F} \ln \left(\frac{I}{I_0^{O_2}} \right) \quad (27)$$

where α_c -charge transfer coefficient of the cathode. Cathode exchange current density is

$$I_0^{O_2} = I_{0,ref}^{O_2} \left(\frac{c_{L,O_2}}{c_{L,ref}^{O_2}} \right) \quad (28)$$

where $I_{0,ref}^{O_2}$ -reference current density at reference concentration $c_{L,ref}^{O_2}$; c_{L,O_2} -concentration of oxygen at gas liquid interface.

Uniform current density is essential for a fuel cell. Local current

Table 3. Operating conditions of DMFC

Channel height	2.0 mm
Channel width	2.0 mm
Operating temperature	80 °C
Anode channel pressure	1 atm
Inlet methanol stream flow rate	2 ^c ml/min; 27.3 ^d ml/min
Inlet methanol concentration	1 M
Inlet carbon dioxide concentration	1 × 10 ⁻⁴ mass fraction
Feeding ratio of oxygen and methanol	$\lambda > \lambda_{min}$
Average current density	2,000 A/m ²

^cCase study 1.

^dCase study 2-4.

density is defined from the cell voltage equation as follows:

$$I = \frac{\sigma}{H} (U_0^{O_2} - U_0^{MeOH} - V_{cell} - |\eta_A| - |\eta_C|) \quad (29)$$

For a fuel cell, reactant stoichiometry is defined as the ratio of the reactant supplied over the reactant theoretically required to produce the current. According to the mass balance, high stoichiometric feed

of air results in a small changing of oxygen concentration in cathode channels and nearly uniform overpotential. In addition to the high feeding ratio, the kinetics of anode reaction has zero order ($n=0$) in the range of high methanol concentration. Local current density Eq. (29) with the above overpotentials Eq. (25) and Eq. (27) is nearly uniform for small variation of concentrations under high feeding ratio. Thus, the assumption of uniform current is valid for high sto-

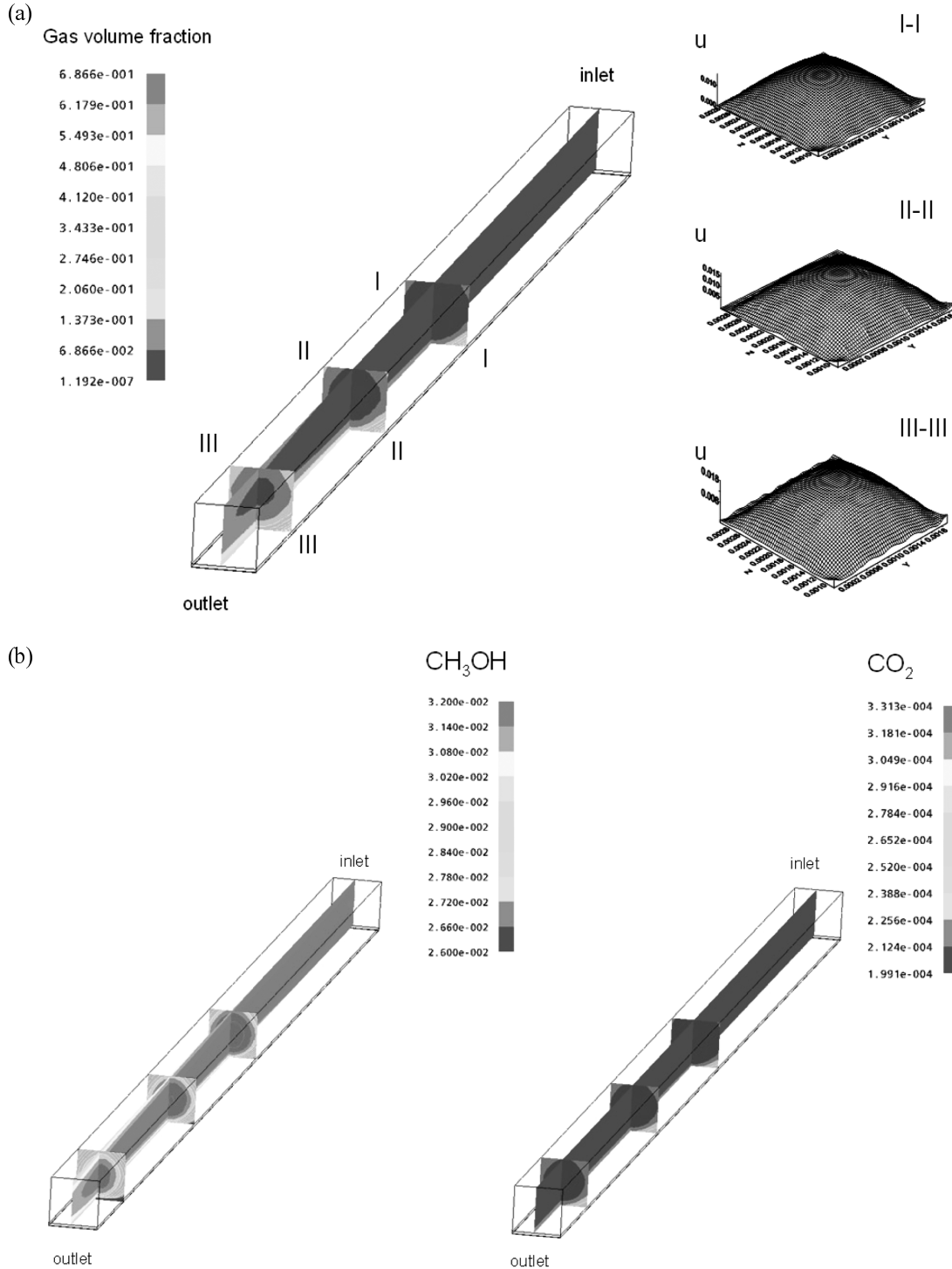


Fig. 2. (a) Development of velocity and gas content profiles along the length of anode channel. (b) Distribution of methanol and carbon dioxide in anode channel predicted by the CFD model. Uniform current density (Table 3).

chiometric feed of air and methanol. As current density is given, we avoid solving conservation equations on the cathode side. The DMFC model with uniform current distribution ($I=\text{const}$) is based on hydrodynamics Eqs. (1)-(8) with boundary conditions Eqs. (9)-(15).

CASE STUDY

The coupled nonlinear transport Eqs. (1)-(8) describe the species and gas evolution in anode channels of the DMFC. The above model equations are coupled closely, so the whole set of equations must be solved simultaneously and iteratively. The DMFC model is implemented in a CFD code to calculate the distribution of velocity, pressure and concentration on anode side for a given flow field design subject to gas management.

Different flow field designs have been reported in literature. A typical design is usually based on parallel or serpentine flow fields. In this study, typical flow fields are evaluated by using flow features such as computed velocity and gas content profiles in anode channels. Table 3 shows flow and operating conditions used in simulations. New flow field designs are developed and evaluated by modifying typical flow field designs.

1. Horizontal Channel

The most simple flow field design is a horizontal channel with 2 mm height and 70 mm length. The developed CFD model with new submodel Eq. (20) is used to simulate the gas evolution in 1.4 cm² DMFC channel under high stoichiometric feed (Table 3). Physicochemical properties of liquid and gas are calculated from equations cited by Wang and Wang [2003]. Fig. 2 shows the development of velocity and gas volume fraction profiles along the anode channel at different cross sections from the inlet. As seen, the velocity profile in the channel corresponds to laminar flow regime. The increase in velocity along the channel is due to volume expansion of

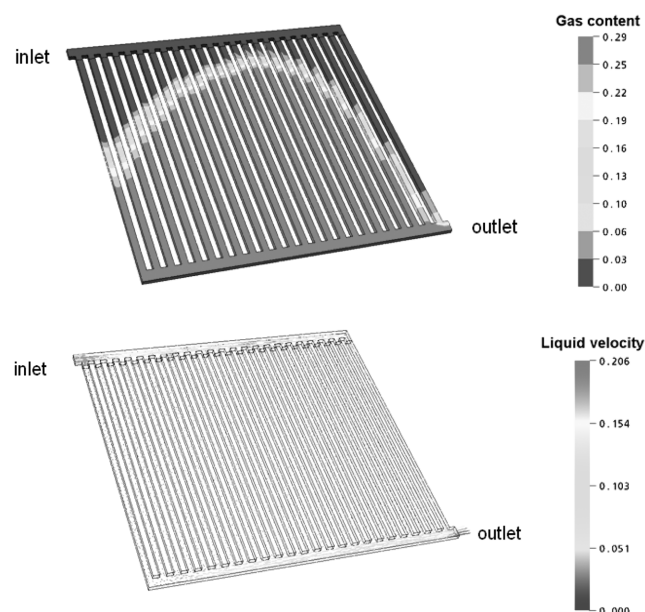


Fig. 3. Gas content and velocity distribution in anode channels for DMFC with parallel flow field. Uniform current density (Table 3).

two phase stream and the increase in gas content. It should be noted that the CFD model predicts a stable wall peak of the gas volume fraction in the channel. The simulation results display symmetrical distributions of gas volume fraction with clear accumulations near walls.

The calculated distribution of velocity, concentration and gas volume fraction agrees with typical trends reported in literature for bubbly flow in pipes and channels.

2. Parallel Flow Field

The parallel flow field is a typical design for a DMFC (Fig. 3). The simulation results in Fig. 3 predict the nonuniform distribution of velocity and gas volume fraction in the anode channels. Gas evolution in parallel channels has a distinguishing feature when low velocity in middle channels leads to the accelerated increase of gas volume fraction along the channels. Higher velocity in the bound-

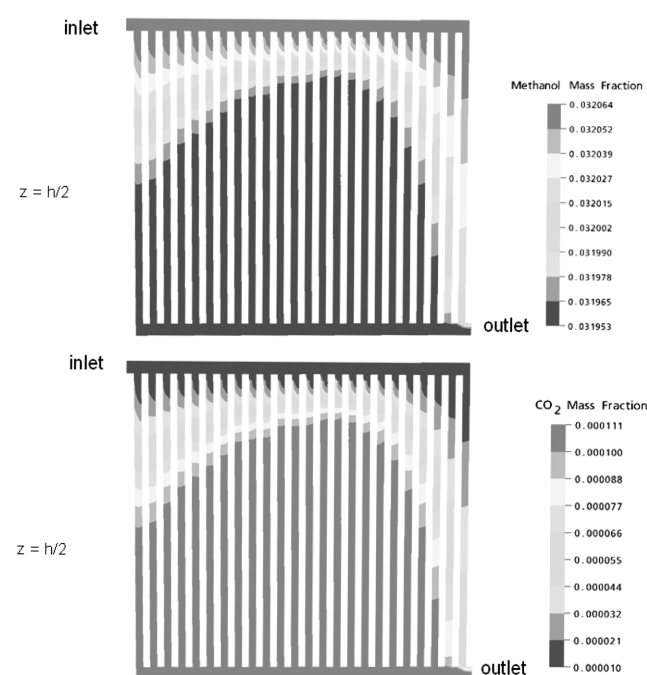


Fig. 4. Distribution of methanol concentration in anode channels for DMFC with parallel flow field. Uniform current density (Table 3).

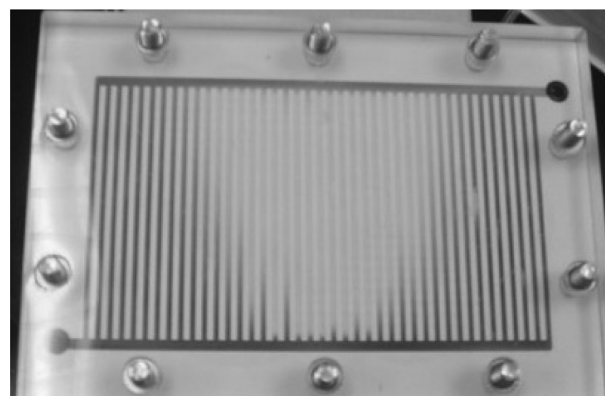


Fig. 5. Tracer distribution in parallel flow field in the case of single-phase flow in a transparent dummy cell.

ing channels compared to that in middle channels leads to the lower increase of gas content along the channels.

Fig. 4 shows a cross section of anode channels with distribution of methanol and carbon dioxide. As seen in Fig. 3 and Fig. 4, flow distribution affects concentration and volume fraction profiles in the anode channel.

Similar distribution of the velocity profile was also observed from the experiment with transparent dummy cell as shown in Fig. 5. The main drawback of the parallel flow field design is that stagnant zones and a reverse flow occur in anode channels under the certain operating conditions. Redistribution of gas volume fraction leads to the accelerated bubble growth and channel blocking in these zones.

3. Modified Parallel Flow Field

A simple way of improving the velocity profile is to increase the flow path in channels. A new modification of the parallel flow field is presented in Fig. 6. The channels are combined to make a long flow path. Fig. 6 and Fig. 7 predict flow maldistribution and formation of stagnant zone. As seen, liquid flow rate in channels increases with distance from inlet section. High concentration of carbon dioxide results in intensive gas evolution in first two channels from the inlet section. The simulation results indicate that nonuniform flow distribution and channel blocking occur in the new design with modified parallel flow field. This modification is not suitable for gas management in the DMFC.

4. Serpentine Flow Field

The most widely used design is serpentine flow field as shown in Fig. 8. Due to long channels, serpentine flow-fields have high pressure drops between the inlet and outlet. Simulation results also reveal specific stagnant zones located at the corners where bubbles may increase in size and block the reactant flow in the channel. It should be noted that flow fields in Fig. 6 and Fig. 8 have the same ele-

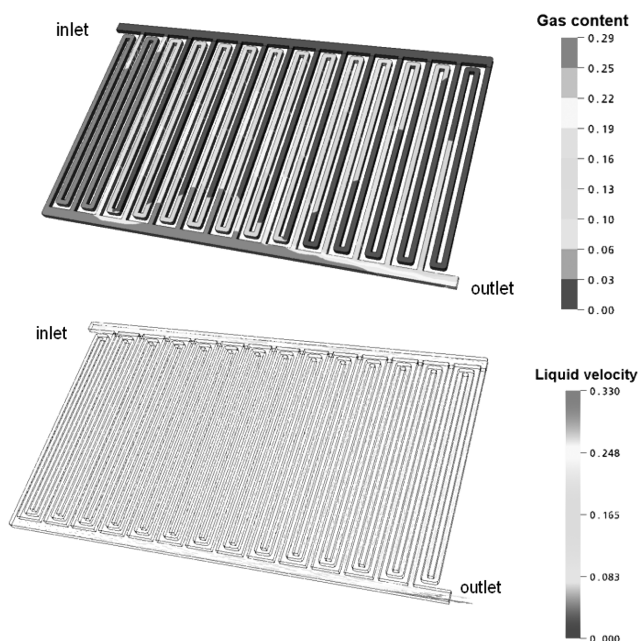


Fig. 6. Gas content and velocity distribution in anode channels for DMFC with modified parallel design. Uniform current density (Table 3).

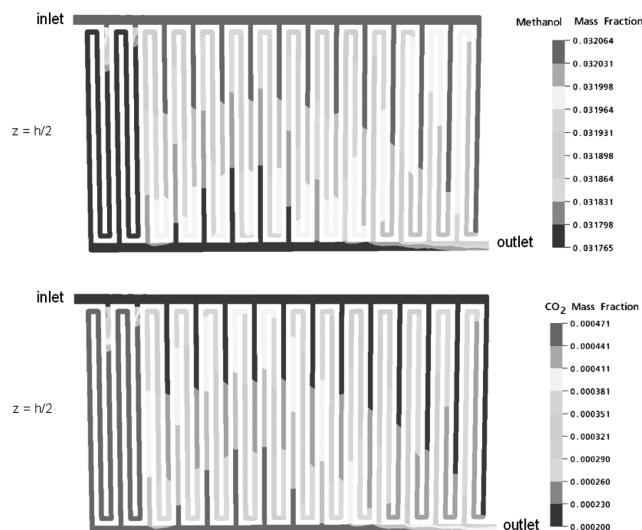


Fig. 7. Distribution of methanol concentration in anode channels for DMFC with modified parallel flow field. Uniform current density (Table 3).

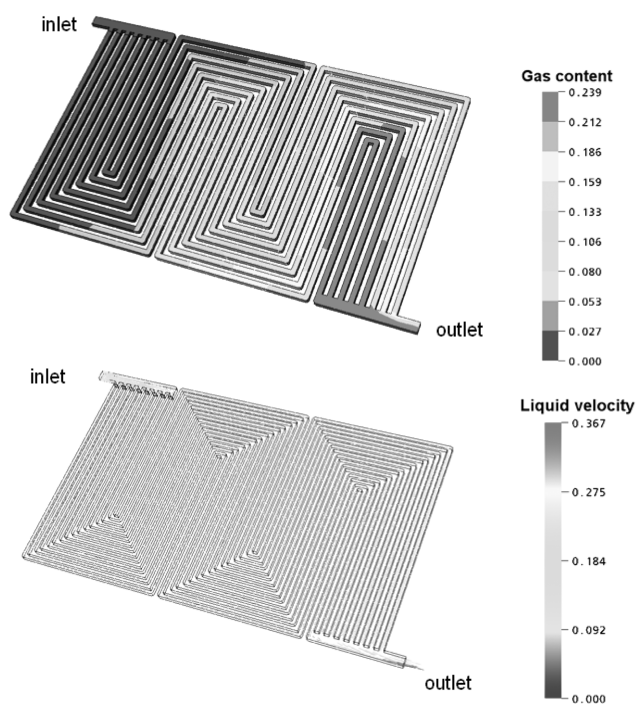


Fig. 8. Gas content and velocity distribution in anode channels for DMFC with serpentine design. Uniform current density (Table 3).

ment in design when a gas-liquid stream in channels sharply changes the flow direction. Simulation results show that the sharp change of flow direction in the channel is a critical point for gas evolution. In addition, stagnant zones and channel blocking phenomena may occur in these critical points.

Taking into account the results from the experiments and simulations, different modifications of serpentine design are developed by using multi-inlet and outlet [Lim et al., 2005]. The modified designs provide a high average velocity and nearly uniform distribution of

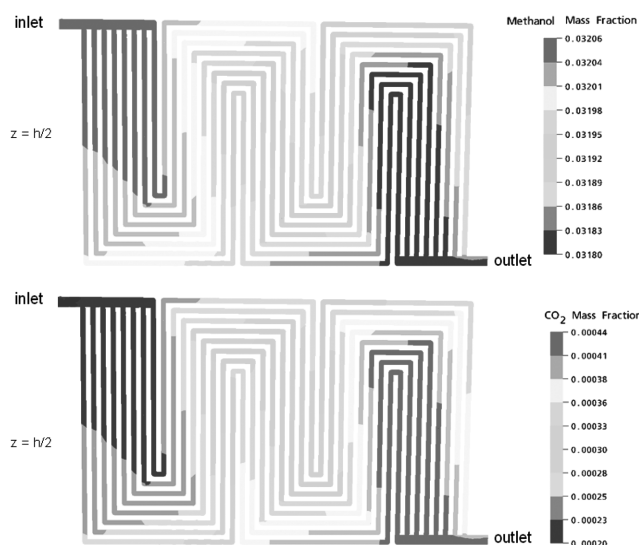


Fig. 9. Distribution of methanol concentration in anode channels for DMFC with serpentine flow field. Uniform current density (Table 3).

reactants in channels. However, the modifications of serpentine flow field still have some difficulties in gas management related to stagnant zones and high pressure drop.

RESULTS AND DISCUSSION

Gas management depends on various parameters, e.g., material properties, cell design and operating conditions. The presence of large gas slugs reduces the free area for the flow and penetration of reactants to the catalyst layer. Channel blocking restricts the supply of reactants to the catalyst layer and hence leads to deterioration in the cell electrical performance. The efficient removal of carbon dioxide is an important factor in DMFC design.

The main objective of gas management is to determine a DMFC flow field design and operating conditions providing uniform distribution of liquid without gas accumulation in channels. Utilization of empirical correlations restricts the application of conventional two-phase model in a new flow field design for gas management in a DMFC. We developed an improved two-phase model of DMFC without using empirical correlations for interface mass transfer. In contrast to Wang and Wang [2003], we used a new equilibrium sub-model for mass source and interphase transfer in anode channels. Uniform current distribution ($I=\text{const}$) under high stoichiometric feed allows us to consider only hydrodynamics and gas evolution on the anode side. This study shows application of the CFD model for exploring gas evolution in DMFC with typical flow fields. Simulation of gas evolution in a horizontal channel of 1.4 cm^2 DMFC indicates that velocity trends to form a fully developed laminar profile. Distribution of velocity and gas volume fraction in the horizontal channel agrees well with trends reported in literature for bubbly flows in channels and pipes.

Simulation results reveal that typical flow fields (parallel and serpentine) have problem areas which lead to ineffective gas removal under certain operating conditions. The simple modification of typical flow field by using multiple inlet and outlet or changing the flow

path is inefficient for gas management. The proposed two-fluid model includes the main factors and it is valuable for gas management in DMFC design. The CFD model can be extended to complete fuel cell model taking into account anode and cathode electrochemical reactions in case of non-uniform current distribution.

CONCLUSION

A CFD-based two-fluid model is developed for gas management in a DMFC design under high stoichiometric feed. The improved two-phase model allows studying gas evolution in DMFC with different flow fields without using empirical correlations. Typical flow field designs such as parallel and serpentine flow fields are simulated and evaluated by using the CFD model. Computed velocity and gas volume fraction distributions are visualized to evaluate the characteristics of flow fields. This study reveals that the parallel flow field design is inefficient for gas management in the DMFC. The newly developed CFD based two-phase model is valuable in flow field design for a DMFC to improve gas management.

ACKNOWLEDGMENTS

This work was supported by a grant from Korean Federation of Science and Technology Societies and Korean Science and Engineering Foundation.

NOMENCLATURE

C	: mass fraction [kg kg^{-1}]
D_{eff}	: effective diffusion coefficient [$\text{m}^2\text{ s}^{-1}$]
F	: Faraday constant [C mol^{-1}]
G	: gas flow rate [kg s^{-1}]
g	: acceleration [m s^{-2}]
k	: permeability of porous material [m^2]
K	: distribution of the components [-]
L	: molar flow rate [mol s^{-1}]
H	: membrane thickness [m]
I	: current [A m^{-2}]
h	: channel height [m]
M	: molecular weight [kg mol^{-1}]
N	: mass flux [$\text{kg m}^{-2}\text{ s}^{-1}$]
P	: pressure [Pa]
R	: gas constant [$\text{J mol}^{-1}\text{ K}^{-1}$]
S	: area [m^2]
T	: temperature [K]
u	: velocity [m s^{-1}]
$U_0^{O_2}$: thermodynamic potential of oxygen reduction [V]
U_0^{MeOH}	: thermodynamic potential of methanol oxidation [V]
V_{anode}	: volume of anode channels [m^3]
V_{cell}	: cell voltage [V]
x	: molar fraction in liquid phase [mol mol^{-1}]; coordinate [m]
y	: molar fraction in gas phase [mol mol^{-1}]; coordinate [m]
z	: coordinate [m]

Greek Letters

α	: transfer coefficient
ε_G	: gas content [$\text{m}^3\text{ m}^{-3}$]

- γ : local fractional vaporization; kinetic factor [-]
 γ_c : advection correction factor [-]
 ρ : density [kg m^{-3}]
 Γ_G : source of mass in gas phase [$\text{kg m}^{-3} \text{s}^{-1}$]
 σ : ionic conductivity of membrane [$\text{m } \Omega^{-1}$]
 ψ : coefficient [$\text{mol m}^{-3} \text{s}^{-1}$]
 μ : viscosity [Pa s]
 η : overpotential [V]
 λ : feeding ratio of air and methanol [-]

Subscripts

- i : component
 in : inlet
 out : outlet
 L : liquid
 G : gas
 A : anode
 C : cathode
 eff : effective
 mix : mixture
 DL : diffusion layer
 ref : reference
 t : total
 s : interface; solid

Superscript

- k : component (MeOH, CO₂, H₂O)

REFERENCES

- Argyropoulos, P., Scott, K. and Taama, W. M., "Carbon dioxide evolution patterns in direct methanol fuel cells," *Electrochimica Acta*, **44**, 3575 (1999).
- Argyropoulos, P., Scott, K. and Taama, W. M., "Modeling pressure distribution and anode/cathode streams vapor-liquid equilibrium composition in liquid feed direct methanol fuel cells," *Chemical Engineering Journal*, **78**, 29 (2000).
- Baxter, S. F., Battaglia, V. S. and White, R. E., "Methanol fuel cell model: Anode," *Journal of the Electrochemical Society*, **146**, 437 (1999).
- Bewer, T., Beckmann, T., Dohle, H., Mergel, J. and Stolten, D., "Novel method for investigation of two-phase flow in liquid feed direct methanol fuel cells using an aqueous H₂O₂ solution," *Journal of Power Sources*, **125**, 1 (2004).
- Danilov, V. A., Lim, J., Moon, I., and Choi, K. H., *A CFD-based Two-fluid Model for a DMFC*, AIChE Annual Meeting, October 30 - November 4, Cincinnati, Ohio (2005).
- Geiger, A., Lehmann, E., Vontobel, P. and Scherer, G. G., *Direct methanol fuel cell—in situ investigation of carbon dioxide patterns in anode flow fields by neutron radiography*, Scientific Report 2000, Volume V, p. 86-87, ed. by: C. Daum and J. Leuenberger, Switzerland, <http://www1.psi.ch/>
- Kim, M. C., Kim, K. Y. and Kim, S., "Two phase visualization by electrical impedance tomography with prior information," *Korean J. Chem. Eng.*, **20**, 601 (2003).
- Kulikovsky, A. A., "Model of the flow with bubbles in the anode channel and performance of a direct methanol fuel cell," *Electrochemistry Communications*, **7**, 237 (2005).
- Lee, S., Kim, D., Lee, J., et al., "Comparative studies of a single cell and a stack of direct methanol fuel cells," *Korean J. Chem. Eng.*, **22**, 406 (2005).
- Lim, J., Danilov, V. A., Cho, Y., Choi, K., Chang, H. and Moon, I., *Flow field design for gas management in a direct methanol fuel cell with a bipolar plate*, in: Proceeding of PSE ASIA (2005).
- Pak, C., Lee, S. J., Lee, S. A., et al., "The effect of two-layer cathode on the performance of the direct methanol fuel cell," *Korean J. Chem. Eng.*, **22**, 214 (2005).
- Sokolichin, A., Eigenberger, G., Lapin, A. and Lübbert, A., "Dynamic numerical simulation of gas-liquid two-phase flows," *Chem. Eng. Sci.*, **52**, 611 (1997).
- Sundmacher, K. and Scott, K., "Direct methanol polymer electrolyte fuel cell: Analysis of charge and mass transfer in the vapor-liquid-solid system," *Chem. Eng. Sci.*, **54**, 2927 (1999).
- Sundmacher, K., Schultz, T., Zhou, S., Scott, K., Ginkel, M. and Gilles, E. D., "Dynamics of the direct methanol fuel cell (DMFC): Experiments and model-based analysis," *Chem. Eng. Sci.*, **56**, 333 (2001).
- Triplett, K. A., Ghiaasiaan, S. M., Abdel-Khalik, S. I., LeMouel, A. and McCord, B. N., "Gas-liquid two-phase flow in microchannels Part II: Void fraction and pressure drop," *International Journal of Multiphase Flow*, **25**, 395 (1999).
- Wang, Z. H. and Wang, C. Y., "Mathematical modeling of liquid-feed direct methanol fuel cells," *Journal of The Electrochemical Society*, **150**, A508 (2003).
- Wang, Z. H., Wang, C. Y. and Chen, K. S., "Two-phase flow and transport in the air cathode of proton exchange membrane fuel cells," *Journal of Power Sources*, **94**, 40 (2001).
- Yang, H. and Zhao, T. S., "Effect of anode flow field design on the performance of liquid feed direct methanol fuel cells," *Electrochimica Acta*, **50**, 3243 (2005).
- Yang, H., Zhao, T. S. and Cheng, P., "Gas-liquid two-phase flow patterns in a miniature square channel with a gas permeable sidewall," *International Journal of Heat and Mass Transfer*, **47**, 5725 (2004).
- Yang, H., Zhao, T. S. and Ye, Q., "Pressure drop behavior in the anode flow field of liquid feed direct methanol fuel cells," *Journal of Power Sources*, **142**, 117 (2005).